CHEMISTRY OF MATERIALS
Article

Chem. Mater. **2010,** *22,* 379–385 379
DOI:10.1021/cm902819x

Conformal Growth of Organic Luminescent Planar Defects within Artificial Opals

Francisco J. Aparicio,† Gabriel Lozano,† Iwona Blaszczyk-Lezak, Ángel Barranco,* and Hernán Míguez*

Instituto de Ciencia de Materiales de Sevilla (CSIC-US), Avenida Américo Vespucio s/n, Isla de La Cartuja, 41092 Sevilla, Spain. † F.J.A. and G.L. contributed equally to this work.

Received September 9, 2009. Revised Manuscript Received November 16, 2009

Herein, we present the result of combining, for the first time, the techniques of colloidal self-assembly and plasma-enhanced chemical vapor deposition to create a novel, high-quality, purely organic active photonic crystal structure of controlled optical properties. We show a fast, reliable, and accurate procedure to introduce two-dimensional luminescent organic defect layers within artificial polystyrene opals via a versatile room-temperature remote plasma deposition process. This method is gentle enough to allow highly conformal growth on polystyrene microspheres without altering their morphology or the ordered arrangement that they form. The luminescent organic layer behaves both as an optical dopant, causing the opening of transmission windows within the forbidden frequency interval of the lattice, and as an optically active material, whose emission can be tailored by the photonic environment.

1. Introduction

The controlled introduction of defects within photonic crystals has attracted great attention since the early days of the field.[1] The reason lies mainly in the interest in carefully engineering defect states within the photonic gap of such lattices, to attain waveguides of higher performance or slow propagation modes.[2] Several techniques have also been applied to create both line and planar defects within solid self-assembled photonic crystals made of spherical colloids that are also known as artificial opals.[3] Since polymer defect lines in the bulk of a silica opal were first achieved using a multiphoton confocal laser to selectively induce polymerization of the embedded monomer,[4] different motifs have been devised and realized within colloidal crystals, using a wide variety of techniques,[5−7] such as direct laser writing,[8] electron beam lithography,[9,10] photolithography,[11,12] or via modifications of the method originally proposed.[13] Significantly, light transmission through linear air defect channels built up in a silicon inverse opal[14,15] structure has recently been demonstrated.[16]

To date, few successful approaches have also been taken up to introduce planar defects in artificial opals. A layer of spheres of an arbitrary diameter can be introduced within the bulk of an opal by combining colloidal crystal planarization and Langmuir−Blodgett techniques.[17] A combination of convective self-assembly and silicon oxide chemical vapor deposition[18] has been used to create a slab sandwiched between two opal films.[19,20] A procedure based on spin coating has also

*Authors to whom correspondence should be addressed. E-mail addresses: hernan@icmse.csic.es (H.M.) and angelbar@icmse.csic.es (A.B.).

(1) Yablonovitch, E.; Gmitter, T. J.; Meade, R. D.; Rappe, A. M.; Brommer, K. D.; Joannopoulos, J. D. *Phys. Rev. Lett.* **1991**, *67*, 3380.
(2) Joannopoulos, J. D.; Villeneuve, P. R.; Fan, S. *Nature* **1997**, *386*, 143.
(3) Jiang, P.; Bertone, J. F.; Hwang, K. S.; Colvin, V. L. *Chem. Mater.* **1999**, *11*, 2132.
(4) Lee, W.; Pruzinsky, S. A.; Braun, P. V. *Adv. Mater.* **2002**, *14*, 271.
(5) Arsenault, A.; Fleischhaker, F.; von Freymann, G.; Kitaev, V.; Míguez, H.; Mihi, A.; Tétreault, N.; Vekris, E.; Manners, I.; Aitchison, S.; Perovic, D.; Ozin, G. A. *Adv. Mater.* **2006**, *18*, 2779.
(6) Braun, P. V.; Rinne, S. A.; García-Santamaría, F. *Adv. Mater.* **2006**, *18*, 2665.
(7) Yang, Q.; Wang, L.; Zhao, X. S. *Adv. Funct. Mater.* **2007**, *17*, 3695.
(8) Tétreault, N.; Míguez, H.; Yang, S. M.; Kitaev, V.; Ozin, G. A. *Adv. Mater.* **2003**, *15*, 1167.
(9) Juárez, B. H.; Golmayo, D.; Postigo, P. A.; López, C. *Adv. Mater.* **2004**, *16*, 1732.
(10) Jonsson, F.; Sotomayor Torres, C. M.; Seekamp, J.; Schniedergers, M.; Tiedemann, A.; Ye, J.; Zentel, R. *Microelectron. Eng.* **2005**, *429*, 78.
(11) Vekris, E.; Kitaev, V.; von Freymann, G.; Perovic, D. D.; Aitchison, J. S.; Ozin, G. A. *Adv. Mater.* **2005**, *17*, 1269.
(12) Yan, Q. F.; Zhou, Z. C.; Zhao, X. S.; Chua, S. J. *Adv. Mater.* **2005**, *17*, 1917.
(13) Jun, Y. H.; Leatherdale, C. A.; Norris, D. J. *Adv. Mater.* **2005**, *17*, 1908.
(14) Blanco, A.; Chomski, E.; Grabtchak, S.; Ibisate, M.; John, S.; Leonard, S. W.; López, C.; Meseguer, F.; Míguez, H.; Mondia, J. P.; Ozin, G. A.; Toader, O.; van Driel, H. M. *Nature* **2000**, *405*, 437.
(15) Vlasov, Y. A.; Bo, X. Z.; Sturm, J. C.; Norris, D. J. *Nature* **2001**, *414*, 289.
(16) Rinne, S. A.; García-Santamaría, F.; Braun, P. V. *Nat. Photonics* **2008**, *2*, 52.
(17) Zhao, Y.; Wostyn, K.; de Schaetzen, G.; Clays, K.; Hellemans, L.; Persons, A.; Szekeres, M.; Schoonheydt, R. A. *Appl. Phys. Lett.* **2003**, *82*, 3764.
(18) Míguez, H.; Tetreault, N.; Hatton, B.; Yang, S. M.; Perovic, D.; Ozin, G. A. *Chem. Commun.* **2002**, 2736.
(19) Palacios-Lidón, E.; Galisteo-López, J. F.; Juárez, B. H.; López, C. *Adv. Mater.* **2004**, *16*, 341.
(20) Tétreault, N.; Mihi, A.; Miguez, H.; Rodriguez, I.; Ozin, G. A.; Meseguer, F.; Kitaev, V. *Adv. Mater.* **2004**, *16*, 346.
(21) Pozas, R.; Mihi, A.; Ocaña, M.; Míguez, H. *Adv. Mater.* **2006**, *18*, 1183.

© 2009 American Chemical Society
Published on Web 12/21/2009

been applied to build, in the first place, embedded layers of nanoparticles,[21] and extended later as a generic method for a variety of materials.[22] This has allowed the observation of slow light modes in controlled defects built in self-assembled photonic crystals for the first time.[23] Transfer printing has also been used to place a polymer multilayer of controlled thickness on top of an opal film, with a second opal being grown on top of it afterward.[24] In this latter case, the optical effects associated with the presence of defects, such as sharp dips (peaks) observed in the reflectance (transmittance) spectra at stop band frequencies, can be precisely tuned through externally induced changes of the polymer material of which the defect is made. These structures also offer the possibility to modify the emission of optically active defect slabs embedded within them. In this regard, only one relevant precedent work has reported on the lasing properties of a polymer defect layer containing organic dyes molecules sandwiched between two flexible self-assembled photonic crystals.[25] To achieve this, a fluid mixture of an oligomer, a curing agent, and dye molecules was infiltrated between two colloidal crystals that had been previously stabilized by infiltration of polydimethilsyloxane (PDMS), which endows mechanical stability and flexibility to the lattice and prevents the luminescent molecules to flow outside the defect layer. A photopolymerization process is then induced by exposure to UV radiation to stabilize the defect layer. This procedure results in high-quality photonic structures in which, unfortunately, the refractive index contrast has been largely reduced, because of the infiltration of PDMS within the crystals, which diminishes its scattering strength and, thus, the magnitude of the localization effects associated with the presence of a defect layer.

Here, we present a fast, reliable, and accurate procedure to create two-dimensional luminescent organic defect layers in artificial opals preserving the photonic strength of the lattice. The planar defect is formed by a versatile, room-temperature, remote plasma deposition process that can be used to create mechanically stable and nonsoluble coatings of a wide variety of organic compounds. The process is gentle enough to allow highly conformal growth on polystyrene microspheres without altering their morphology or the ordered arrangement they form, thus giving rise to purely organic photonic nanostructures. Accurate control of the defect thickness is achieved, which yields control over the spectral position of the defect state introduced in the pseudo-gap of the photonic crystal, because of the breaking of translational symmetry. This resonant mode causes the opening of a narrow transmission window that can be precisely adjusted during the synthesis. The emission properties of the middle layer can be controllably modified through the structural properties of the photonic environment in which it is embedded.

Despite the great amount of materials that can be grown using plasma-based techniques,[26] to date, they have only been applied for the processing of self-assembled photonic materials as a means to selectively remove an ordered organic matrix that had been used to either mold a guest material or hold a more-complex structure together.[27] Most plasma processes are too aggressive, both chemically and thermally, for organic materials, such as polystyrene opals, to resist them. However, they present many advantages that make them extremely desirable to prepare optical coatings, the main ones being probably the strict control of the features achievable at the nanometer scale, the conformal character of the growth, and the great reliability and reproducibility of the process. In our case, we have employed a plasma-enhanced chemical vapor deposition (PECVD) technique developed at our laboratories,[28−30] in which partial polymerization of functional organic molecules is induced by the controlled interaction with a remote microwave plasma. By this methodology, it has been possible to deposit a layer of a luminescent organic solid material directly on a polystyrene artificial opal. The luminescent dye 3-hydroxyflavone (3HF) and adamantane are used as precursors for the synthesis of such films. Since full details are given in the Materials and Methods section, suffices to say here that we have achieved deposition conditions mild enough to leave the photonic crystal substrate unaltered during the process. In addition, the hydrophilic character of the organic thin film surface is achieved by tuning the PECVD parameters at the end of the deposition. This latter process has permitted the deposition of a second layer of opal onto it, giving rise to a photonic crystal in which the translational symmetry is broken by the presence of an intermediate luminescent nanostructured film.

2. Materials and Methods

Fabrication of Colloidal Crystal Films. The growth of colloidal crystals from polystyrene (PS) colloids in deionized water was conducted using a variation of the vertical deposition method developed by Colvin and coworkers.[3] For this purpose, commercial PS colloidal particles (IIKERLAT) with average diameters of 220 and 750 nm (with a polydispersity of ∼3%) were used. The substrates employed were glass microscope slides (12 mm × 76 mm), which were cleaned with doubly distilled

(22) Fleischhaker, F.; Arsenault, A. C.; Schmidtke, J.; Zentel, R.; Ozin, G. A. *Chem. Mater.* **2006**, *18*, 5640.
(23) Galisteo-López, J. F.; Galli, M.; Andreani, L. C.; Mihi, A.; Pozas, R.; Ocaña, M.; Míguez, H. *Appl. Phys. Lett.* **2007**, *90*, 101113.
(24) Tétreault, N.; Arsenault, A. C.; Mihi, A.; Wong, S.; Kitaev, V.; Manners, I.; Míguez, H.; Ozin, G. A. *Adv. Mater.* **2005**, *17*, 1912.
(25) Furumi, S.; Fudouzi, H.; Miyazaki, H. T.; Sakka, Y. *Adv. Mater.* **2007**, *19*, 2067.
(26) Yasuda, H. *Luminous Chemical Vapor Deposition and Interface Engineering*, CRC Press: Boca Raton, FL, 2004
(27) García-Santamaría, F.; Miyazaki, H. T.; Urquia, A; Ibisate, M.; Belmonte, M.; Shinya, N.; Meseguer, F.; López, C. *Adv. Mater.* **2002**, *14*, 1144.
(28) Barranco, A.; Groening, P. *Langmuir* **2006**, *22*, 6719.
(29) Barranco, A.; Aparicio, F. J.; Yanguas-Gil, A.; Groening, P.; Cotrino, J.; González-Elipe, A. R. *Chem. Vap. Deposition* **2007**, *13*, 319.
(30) Blaszczyk-Lezak, I.; Aparicio, F. J.; Borrás, A.; Barranco, A.; Álvarez-Herrero, A.; Fernández-Rodriguez, M.; González-Elipe, A. R. *J. Phys. Chem. C* **2009**, *113*, 431.

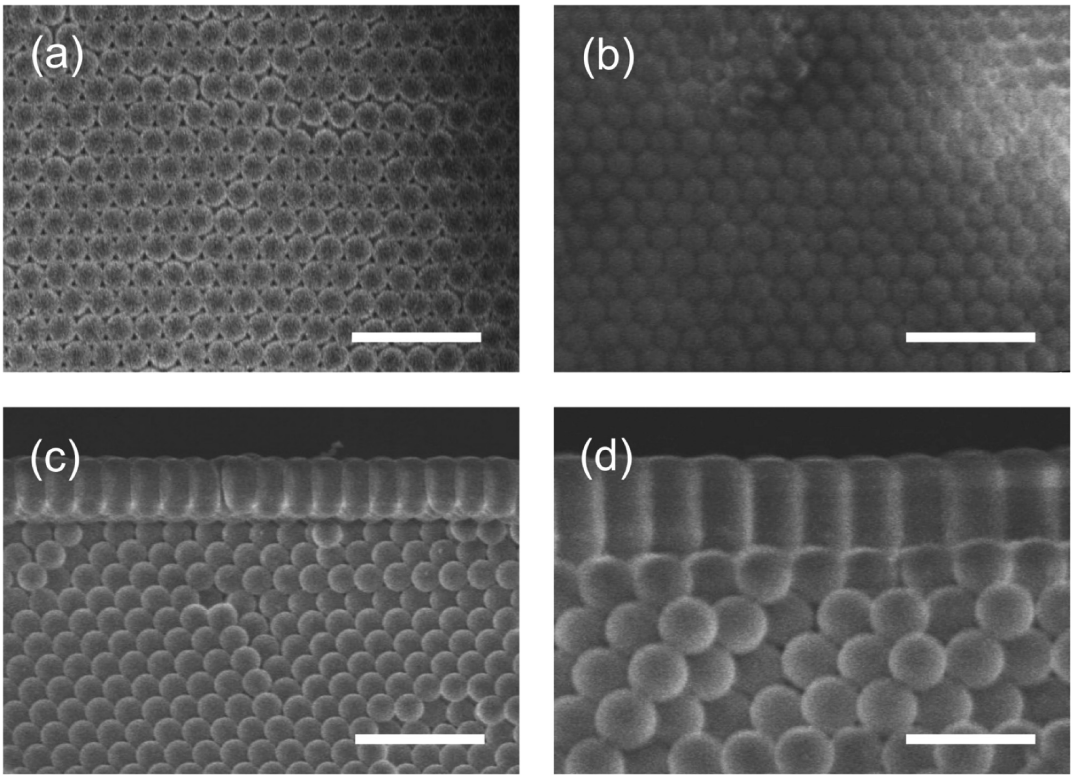

Figure 1. Field-emission scanning electron microscopy (FESEM) images of the stages of the fabrication of a surface defect layer: (a) top surface micrograph of the starting latex colloidal crystal film; (b) top surface of the 2D planar defect layer; and (c) low-magnification micrograph of the cross-section showing the defect layer. Panel d shows the detail of the defect layer. (Scale bars in panels (a)−(c) are 1 μm, and that in panel (d) is 500 nm.)

water, acetone, carbon tetrachloride, and a H_2SO_4/H_2O_2 solution (4:1 volume ratio) before being dried with a N_2 flow. These substrates were dipped into a cylindrical glass beaker (with an inner diameter of ca. 25 mm and a volume of 25 mL) containing the PS colloidal suspensions (15 mL) with a concentration of 0.04 wt %. The beakers then were placed in an oven at 50 °C and water was evaporated for 3 days, with a high-quality colloidal crystal being formed on an area of 12 mm × 16 mm of the substrate. Similar conditions were employed to grow a second colloidal crystal on the hydrophilic surface of the corrugated polymeric thin film deposited by PECVD to create a planar defect embedded in a photonic crystal.

Plasma Polymerization of Organic Layers. The experimental setup used for deposition of the polymeric thin films consists of a vacuum chamber with two zones for the plasma and for the remote deposition. A set of magnets surrounding the plasma chamber sustain a discharge under microwave electron cyclotron resonance (ECR) conditions. The microwave is applied to the plasma chamber through a flat Pyrex window. The system is fitted with a set of Knudsen cells to sublimate the dye in the deposition zone and a precursor dosification system that can be heated. The pressure of the system was controlled by an automatically regulated pressure controller that was connected to a capacitance pressure gauge (Baratron). Argon plasma gas is dosed to the plasma chamber, using a calibrated mass flow controller (MKS). The system was pumped before and after deposition with a turbomolecular pump to achieve a base pressure of $\sim 10^{-7}$ mbar. One-side-polished Si(100) wafers, quartz, slides, and the colloidal crystal films used as substrates were placed in the deposition chamber.

The polymerized thin films were deposited at room temperature by the simultaneous sublimation of 3-hydroxyflavone (3HF) and adamantane powders (Aldrich) in the downstream region of an argon plasma. The film thickness and evaporation rate are controlled using a quartz crystal monitor that has been placed beside the sample holder in the deposition region. Typical growth rates of 2−4 nm/min were achieved by controlling the temperature of both the Knudsen cells for the dye and the dosification system for the adamantane. Using relatively low growth rates, it was possible to control the deposition of ultrathin films efficiently, typically within the range of 20−500 nm. The microwave power was ∼150 W, and the argon pressure was $\sim 1 \times 10^{-2}$ mbar. Artificial opal samples were located ∼6 cm from the plasma source. Additional details of the experimental setup used can be found in refs 28−30. Absorbance and fluorescence spectra of a 3HF−adamantane plasma polymer film that has been grown over quartz are provided as Supporting Information. In addition, a complete study of the properties of the 3-HF−adamantane plasma polymers deposited by this novel process will be presented elsewhere. Films were exposed to an oxygen plasma (240 W, 10^{-3} mbar) by introducing an oxygen flow during ∼3 min at the end of the deposition, to obtain highly hydrophilic

(31) Ostrikov, K. *Rev. Mod. Phys.* **2005**, *77*, 489.

surfaces. Special care was taken not to etch the polystyrene spheres at this stage. Micrographs of top views and cross sections of the different samples prepared were obtained using a Hitachi S5200 field-emission scanning electron microscope.

Optical Spectroscopy. Optical characterization was performed using a Fourier transform infrared spectrophotometer (Bruker, Model IFS-66) that was attached to a microscope and operating both in reflection and transmission mode. For reflectance measurements, an 4× objective with a numerical aperture of 0.1 (light cone angle of ±5.7°) was used to irradiate the sample and collect the reflected light at quasi-normal incidence, with respect to the (111) planes of the colloidal lattice. A spatial filter was used to selectively detect light from 1-mm^2 circular regions of the sample.

Luminescence Spectroscopy. Fluorescence spectra were measured in a Jobin−Yvon Model Fluorolog3 spectrofluorometer that was equipped with a 450 W xenon lamp, using grids of 0.4 and 1 nm for the excitation and emission, respectively. The excitation wavelenght was 350 nm. Fluorescence spectra were measured with slightly modified front-face configuration to collect emission spectra at quasi-normal direction, with respect to the (111) planes of the colloidal lattice. For this analysis, the luminiscent layers were also deposited in quartz slides.

3. Results and Discussion

Figures 1 and 2 show different images of the prepared materials, as viewed using field-emission scanning electron microscopy (FESEM). Figures 1a and 1b display images of the top surface of a polystyrene opal (with an average sphere diameter of 220 nm) before and after being coated with the plasma polymeric thin film, respectively. The coherent corrugation of the colloidal crystal substrate is preserved, which demonstrates the highly conformal deposition of the organic thin film that occurs via the PECVD technique employed. The pictures of the cross section taken at different magnifications, shown in Figures 1c and 1d, revealed that the films develop a columnar structure and that the growth occurs preferentially from the surface of the microspheres upward. Furthermore, the micrograph also shows that the void space existing between the spheres is not preserved in the columnar thin film. These observations suggest that the topmost layer of the opal is acting as a template for the growth of the polymeric nanostructured film. Thus, the deposited organic materials consist in a hexagonal close packing arrangement of oriented organic nanopillars whose surface reproduce conformally the surface of the original opal substrate. Note that the original opal top layer is integrated in the lower part of the cylindrical structures. The diameters of the cylindrical nanopillars are constant, indicating preferential growth perpendicular to the opal surface with a low lateral diffusion of the species (i.e., high sticking coefficients) arriving to the surface during the deposition. In any case, the reduced lateral growth produces the filling of the void space between the nanopillars generating the hexagonal tilling pattern observed in the polymeric surface (cf. Figure 1b). Additional effects responsible of the formation of the oriented nanostructured film are very likely shadowing effects and local inhomogeneities of the plasma sheath that are due to the opal surface topography.[31,32] This type of plasma nanostructured thin films has not been reported so far. Organic thin films grown simultaneously but using flat Si(100) and quartz substrates are continuous and uniform and present a very low surface

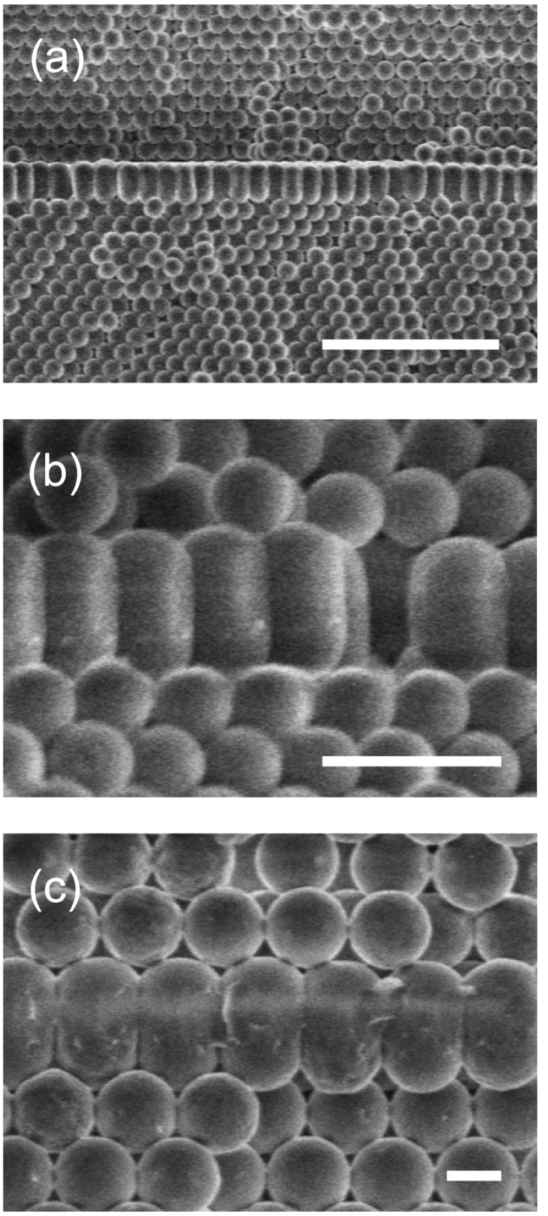

Figure 2. FESEM images of a defect layer embedded between two colloidal photonic crystal films: (a) low-magnification micrograph, showing that the 2D defect layer thickness is uniform over the entire sample; (b, c) closer look at the defect layer. Opals shown in panels (a) and (b) are made of 220-nm polystyrene beads, whereas those presented in panel (c) are made of 750-nm polystyrene beads. (Scale bar in panel (a) is 2 μm, and those in panels (b) and (c) are 500 nm.)

(32) Borrás, A.; Barranco, A.; Espinós, J. P.; Cotrino, J.; Holgado, J. P.; González-Elipe, A. R. *Plasma Processes Polym.* **2007**, *4*, 515.

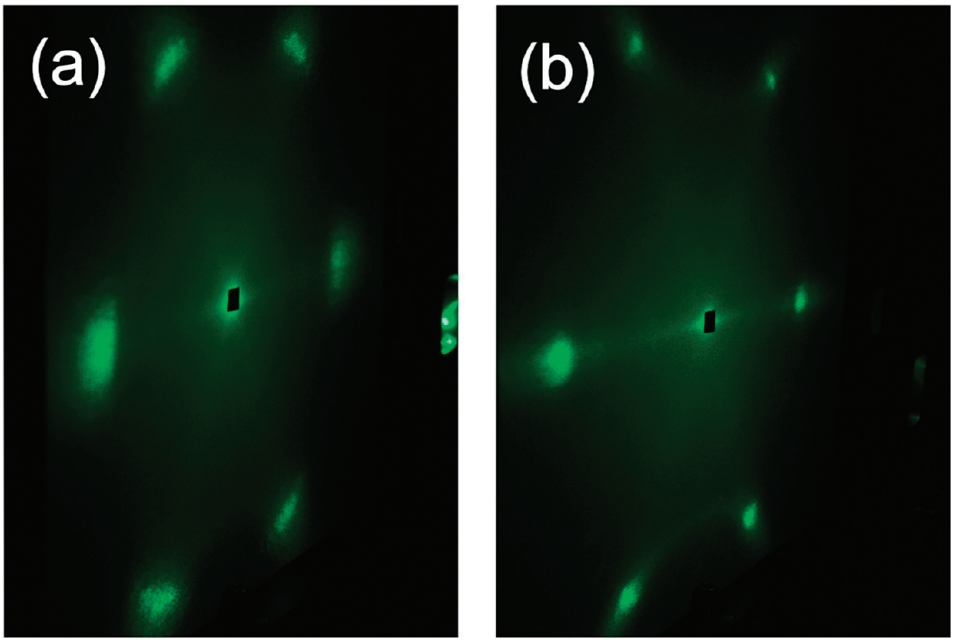

Figure 3. Diffraction patterns of reflected beams projected on a screen parallel to the surface of the samples for $\lambda = 532$ nm: (a) diffracted beams exiting from the surface of a colloidal crystal made of 750-nm-diameter spheres, and (b) diffracted beams emerging from a similar crystal covered by the conformal organic fluorescent layer.

roughness, as it has been observed in other films deposited using this technique.[28−30] Images illustrating the difference between the morphology of the film grown on an array of microspheres and on a flat substrate are provided as Supporting Information. Note that the structure presented herein has some similarities with non-closed-packed hexagonal patterns of hemispherical TiO_2 particles generated by pulsed laser deposition that has been reported very recently.[33]

The sequential deposition of a second artificial opal (with an average sphere diameter of 220 nm) onto the deposited organic layer yields a structure similar to that shown in Figure 2. The periodic corrugation of the intermediate layer favors the growth of a second lattice of long-range structural order, as seen in Figure 2a. Furthermore, the relative orientation of the two crystals, with respect to the original glass substrate, is maintained. Similar structures were created using artificial opals made of spheres of different average diameter, with consistent results in all cases. Figures 2b and 2c display low-magnification images of the cross section of organic planar defects sandwiched between two colloidal crystals made of 220- and 750-nm latex beads, respectively.

The level of accuracy and finesse with which the features of the substrate are reproduced by the PECVD technique employed can also be confirmed by observing the effect of the presence of a coating on the visible optical diffraction typically displayed by assemblies of microspheres with diameters of >400 nm. Pictures of the projection on a screen of the beams diffracted in the reflection medium by both an artificial opal made of 750-nm spheres and the same opal after being coated with a conformal layer of the organic fluorescent film are shown in Figures 3a and 3b, respectively. A $\lambda = 532$ nm laser line impinging normally on their surface was employed for this experiment. The pattern of spots on the screen remained unaltered after the conformal deposition of the luminescent organic layer, which further establishes that the corrugation of the periodic substrate is maintained. In fact, a certain narrowing of the diffraction spot area was observed after the deposition of the outer layer. This indicates that the divergence of the reflected diffracted beams potentially caused by the presence of imperfections in the opal lattice is reduced by the effect of the outer conformal layer.

Breaking of the translational symmetry within photonic crystals creates localized modes. This causes strong variations of the local photon density of states that may be reflected in both the opening of a transmission window in the forwardly forbidden band and, for the case of optically active materials, enhanced emission at wavelengths matching those resonant modes. Figures 4a and 4c display the fluorescence spectra measured for 305- and 515-nm-thick luminescent organic layers, respectively, embedded within artificial opal films made of spheres 220 nm in diameter. For the sake of comparison, the fluorescence spectrum measured from a 515-nm-thick organic layer deposited on a stacking of 750-nm-diameter spheres, for which no photonic effects associated with a stop band at the dye emission frequencies were expected, is also shown. A photoemission enhancement factor (γ) is calculated for each case as the ratio between the fluorescence spectra of the photonic crystal sandwiched organic layer and the reference. For the opal films that are composed of 220-nm-diameter spheres, the fluorescence intensity is higher in the case of crystals that contain a thicker luminescent layer (515 nm thick). For the sake of comparison, fluorescent spectra are normalized

(33) Li, Y.; Sasaki, T.; Shimizu, Y.; Koshizaki, N. *Small* **2008**, *4*, 2286.

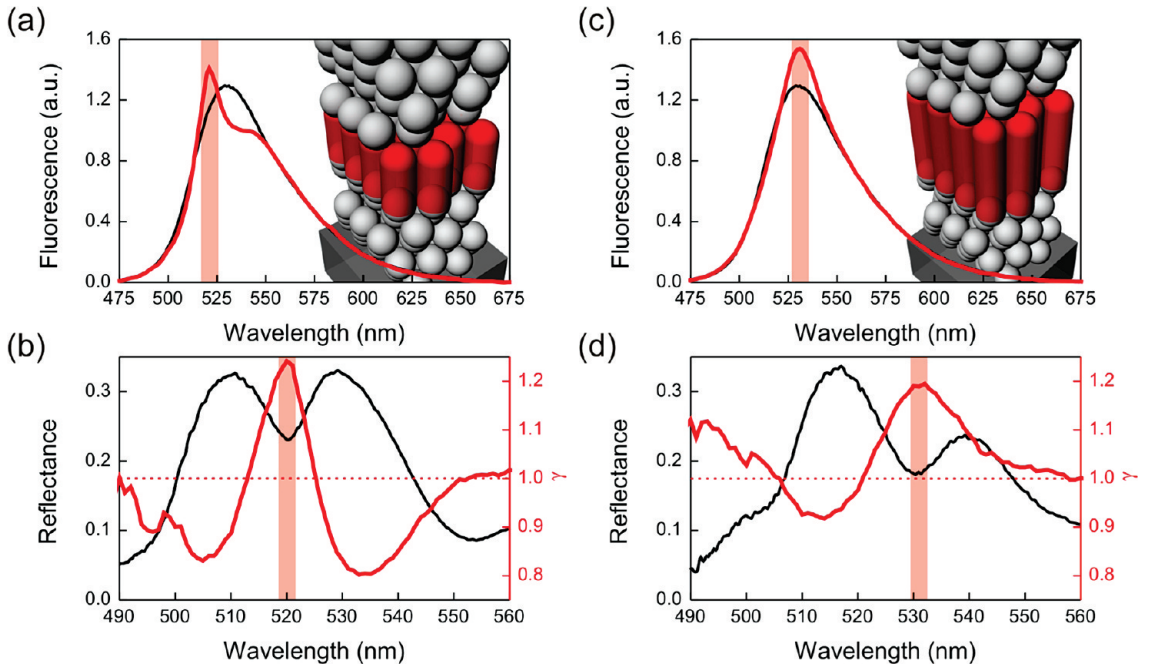

Figure 4. Normalized fluorescent and reflectance spectra obtained from (a, b) a 305-nm-thick and (c, d) a 515-nm-thick defect layer embedded within two artificial opal films made of 220-nm-diameter spheres. Panels (a) and (c) show normalized fluorescence spectra of the layer embedded within a photonic crystal (red line) and of a 515-nm-thick organic layer deposited on a stacking of 750-nm-diameter spheres, for which no photonic effects associated with a stop band at the dye emission frequencies were expected (black line). Panels (b) and (d) show the reflectance spectrum of the defect layer sandwiched between the two colloidal crystal films and the enhancement factor γ, defined as the ratio between the fluorescence spectra presented in panels (a) and (c). (Red dotted line represents the $\gamma = 1$ line.)

at $\lambda = 650$ nm, where no effect of the photonic structure is expected. Both samples were devised to ensure that the lowest stop band of the photonic crystal coincides with the emission band of the solid dye slab, hence forcing any resonant modes due to the presence of a defect layer to overlap with part of such emission band. A transmission window can be clearly detected at $\lambda \approx 520$ nm and $\lambda \approx 530$ nm for the 305- and 515-nm-thick defects, respectively. These reflectance dips at pseudo-gap frequencies are due to the presence of localized modes within the defect layers, for which the emission intensity is expected to be enhanced. Red-shadowed rectangles indicate the spectral position of such localized modes. The enhancement effect was confirmed for both samples whose analysis is presented herein by comparing the spectral behavior of γ with the specular normal reflectance spectrum measured in each case. In both cases, it can be clearly seen that the γ value peaks at those frequencies for which the resonance is detected in the reflectance spectrum. At the same time, it diminishes for those frequencies within the photonic stop band that are spectrally far from those localized modes. It should be remarked that, for the sample used as a reference, no significant modification of the shape of the spectrum is observed, with respect to that attained for the plane parallel dye slabs deposited onto flat substrates (see Figure S2 in the Supporting Information). Reflectance spectrum of reference sample (Figure S3 in the Supporting Information) clearly shows that, for this structure, the lowest-energy photonic pseudo-gap does not spectrally match the emission band of the organic layer. This proves that the variations of the shape of the emission band have a structural origin.

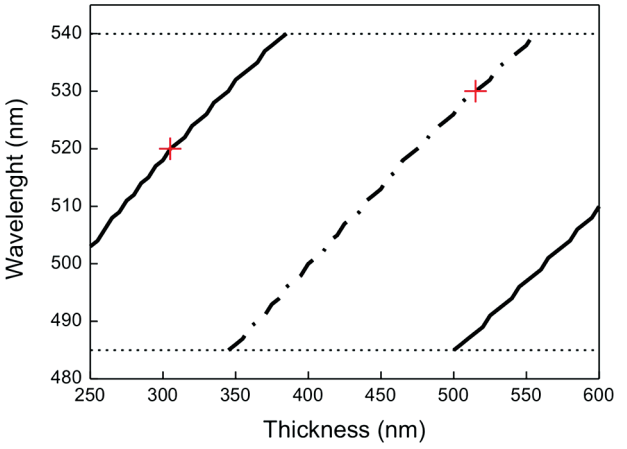

Figure 5. Theoretical dependence between the localized mode associated to the defect state and the thickness of the organic fluorescent layer. Experimental values extracted both from the FESEM characterization and from the fittings of the reflectance spectra presented in Figures 4b−d are plotted as red crosses. Horizontal dotted lines depict the stop-band limits of the infinite crystal.

Results presented in Figure 4 demonstrate that, by changing the deposition time, it is possible to control the thickness of the organic layer acting as an optical dopant and thus tailor the spectral position of the localized mode that it creates. In Figure 5, we compare the experimental values of the defect state for two different intermediate layer thicknesses achieved with the theoretical predictions obtained using a scalar wave approximation.[21] Results are shown for defects embedded within lattices of 13 monolayers each. Experimental data are plotted as red crosses in Figure 5. As reported previously,[20] the defect state sweeps the full width of the peak from the blue end to

the red end as the thickness of the defect increases, and this behavior repeats cyclically. The stop-band edges estimated for the infinite crystal are depicted as horizontal dotted lines in Figure 5.

4. Conclusions

In summary, we have described a fast, reliable, and accurate procedure to create two-dimensional luminescent organic defect layers in artificial opals. A versatile, room-temperature, remote plasma-enhanced chemical vapor deposition has been used to create mechanically stable and nonsoluble coatings. We have proven that the process yields a highly conformal growth that preserves the integrity and the properties of the polystyrene microspheres. The effect of resonant modes, caused by the presence of a middle layer in the photonic crystal, in both reflectance and photoemission spectra, has been confirmed. Our work opens the possibility for integration of these nanostructures in purely organic light-emitting devices in which the optical properties can be precisely controlled.

Acknowledgment. We thank the Spanish Ministry of Science and Innovation for funding provided under grants MAT2008-02166, MAT2007-65764, CONSOLIDER HOPE CSD2007-00007, and FUNCOAT 2010-CSD2008-00023, the Junta de Andalucía for grants FQM3579 and TEP2275, and EU Contract No. 033793 (Phodye). G.L. thanks the Spanish Research Council for funding of his scholarship under the JAE program.

Supporting Information Available: FESEM image of a cross section of an edge of the photonic structure illustrating the different morphology of the dye layer attained when deposited on an array of spheres or on a flat substrate (Figure S1). Normalized absorbance and fluorescence spectra from a flat 3HF-adamantane plasma polymer film grew over quartz (Figure S2). Reflectance spectra obtained from the sample employed as reference (Figure S3). (PDF) This material is available free of charge via the Internet at http://pubs.acs.org.